RESPONSE OF OSTEOBLAST-LIKE CELLS ON TITANIUM SURFACE TREATMENT

Hyun-Ki Roh, D.D.S., M.S.D., Seong-Joo Heo, D.D.S., Ph.D., Ik-Tae Chang, D.D.S., Ph.D., Jai-Young Koak, D.D.S., Ph.D., Jong-Hyun Han, D.D.S., Ph.D.*, Yong-Sik Kim, D.D.S., Ph.D., Soon-Ho Yim, D.D.S., Ph.D.*****

Department of Prosthodontics, Graduate School, Seoul National University

*Yonsei University, Yongdong Sevrance Hospital, **University of Ulsan, Asan Medical Center, ***Sungkyunkwan University, School of Medicine

Statement of problem. Titanium is the most important material for biomedical and dental implants because of their high corrosion resistance and good biocompatibility. These beneficial properties are due to a protective passive oxide film that spontaneously forms on the surface.

Purpose. The purpose of this study was to evaluate the responses of osteoblast-like cells on different surface treatments on Ti discs.

Material and Methods. Group 1 represented the machined surface with no treatment. Group 2 surfaces were sandblasted with 50μm Al_2O_3 under 5 kgf/cm^2 of pressure. Groups 3 and 4 were sandblasted under the same conditions. The samples were treated on a titanium oxide surface with reactive sputter depositioning and thermal oxidation at 600℃ (Group 3) and 800℃ (Group 4) for one hour in an oxygen environment.

The chemical composition and microtopography were analyzed by XRD, XPS, SEM and optical interferometer. The stability of TiO_2 layer was studied by potentiodynamic curve. To evaluate cell response, osteoblast extracted from femoral bone marrow of young adult rat were cultured for cell attachment, proliferation and morphology on each titanium discs.

Results and Conclusion. The results were as follows :

1. Surface roughness values were, from the lowest to the highest, machined group, 800℃ thermal oxidation group, 600℃ thermal oxidation group and blasted group. The Ra value of blasted group was significantly higher than that of 800℃ thermal oxidation group ($P=0.003$), which was not different from that of 600℃ thermal oxidation group ($P<0.05$).
2. The degree of cell attachment was highest in the 600℃ thermal oxidation group after four and eight hours ($P<0.05$), but after 24 hours, there was no difference among the groups ($P>0.05$).
3. The level of cell proliferation showed no difference among the groups after one day, three days, and seven days ($P>0.05$).
4. The morphology and arrangement of the cells varied with surface roughness of the discs.

Key Words

Ti surface treatment, Microtopography analysis, Osteoblast response

※ This work was supported by a grant from the Korean Health 21 R&D project, Ministry of Health & Welfare, Republic of Korea(02-PJ3-PG6-EV11-0002).

Titanium is the most important material for biomedical and dental implants because of its relatively high corrosion resistance and good biocompatibility. These beneficial properties are due to a protective passive oxide film that spontaneously forms on the surface. It has been suggested that the physiochemical and dielectric properties of the oxide film play a decisive role in determining the biocompatibility of the implants, and that the special osseointegration feature of titanium oxide films is responsible for a direct bone-titanium contact and strong bonding.

The natural passive film on titanium is formed in many aqueous solutions, air, or other oxygen-containing environments, is normally only a few nanometers thick, and consists essentially of titanium dioxide. Despite frequent report of negligible corrosion rates of titanium in vitro, there is increasing evidence that titanium may be released extensively in vivo, and, under certain conditions, may accumulate in adjacent tissues or be transported to distant organs. These observations indicate that the biological environment may be quite aggressive towards titanium or its thin oxide film. Also, oxide growth and the incorporation of ions into the titanium oxide film have been observed in human bodies. Both the release of titanium and surface oxide growth are of great importance for the biocompatibility of titanium implant materials.

The morphology of an implant surface, including microtopography and roughness, has been shown to be related to successful bone fixation.[1,2] In addition, the manufacturing process used to achieve the surface texture, either chemical[3] or mechanical,[4] also influences clinical success. Currently, the clinical use of titanium implants varies with respect to surface roughness and composition. Generally speaking, bone forms more readily on a rough surface, whereas fibrous connective tissue is found more frequently on a smooth surface.[5]

In vitro studies have provided some insights into the response of specific cell types to surface properties. It is clear that the degree of surface roughness affects cell response. In particular, osteoblast-like cells exhibit roughness-dependent phenotypic characteristics, tending to attach more readily to surfaces with a rougher microtopography.[6,7] Moreover, they appear to be more differentiated on rougher surfaces with respect to morphology, extracellular matrix synthesis and alkaline phosphatase specific activity.[8,9] The morphology of the surface also plays a role. A variety of cells can orient themselves in the grooves of micromachined surfaces.[10,11] Depending on the degree of roughness, these cells may actually see the grooves as smooth. On a randomly rough surface created by grit blasting or chemical etching, cells may form different focal attachments, which result in a phenotype that is distinct from that seen on the grooved surface with the same degree of roughness. Several studies have shown that even subtle differences in surface composition, including Ti oxide crystallinity, can modify cell response, even when surface roughness is held constant.[12,13]

For this study, smooth surfaces were obtained by machining, rough surfaces were obtained by sandblasting, and compositional change of the TiO_2 layer was achieved by thermal oxidation with TiO_2 reactive sputter deposition. This vacuum deposition technique produces high quality coatings with good bonding to either smooth or rough titanium surfaces, but it usually requires a heat treatment in a controlled atmosphere in order to attain high crystallinity. To determine whether the composition of the surface or microtopography are important variables for determining osteoblastic phenotype, we examined the response of osteoblast cells on various treated titanium disc surfaces.

MATERIALS AND METHODS

2.1. Titanium disc preparation and characterization

Titanium discs were fabricated from a bar of

commercially pure titanium (Ti:medical grade 2. ASTM). The chemical composition was provided by the supplier and was not verified prior to surface preparation. All samples were air dried and sterilized with ethylene oxide gas for 24 hours.

The experiment was composed of four groups. Group 1 represented the machined surface with no treatment. Group 2 surfaces were sandblasted with 50μm Al_2O_3 under 5 kgf/cm^2 of pressure. Groups 3 and 4 were sandblasted under the same conditions. The samples were treated on a titanium oxide surface with reactive sputter depositioning and thermal oxidation at 600℃ (Group 3) and 800℃ (Group 4) for one hour in an oxygen environment.

The reactive sputter deposition was carried out in an environment targeting TiO_2, 300 watt power, 15 sccm total gas flow, and 5 mTorr working pressure. The gas flow was maintained at 5 sccm O_2 and 10 sccm argon (Fig. 1). After 300 minutes of sputter deposition, the specimens underwent additional annealing by thermal oxidation in an O_2 environment for one hour (Fig. 2). Representative disks from each group were subjected to surface analysis.

2.1.1 SEM analysis

The surface microtopography of the discs was examined using a scanning electron microscope (S-800, Hitachi, Japan). Samples from each group were examined at 200 to 700 × magnification.

2.1.2 Optical interferometer analysis

The optical interferometer is the instrument used to analyze light interference phenomena. Incident flux is divided into reference flux and measurement flux, and they incident reference surface and measuring surface respectively. The two fluxes, then, combine together to develop an interference pattern that represents the optical path difference. This pattern is captured by a CCD camera and is analyzed using an image process and analyzing method that produces a three dimensional image. We used the Optical Dimensional Metrology Center (Intek Engineering, Korea) (Fig. 3).

Ra : This is the arithmetic mean of the absolute values of the surface departures from a mean plane within the sampling area. The parameter is measured in μm and is a general and commonly used parameter.

Rt : This extreme value is the distance between the highest peak and the lowest valley within the sampling area, and is measured in μm.

Rsk : Skewness is the measure of the symmetry of surface deviations about the mean plane (e.g. a negatively skewed surface has more valleys than peaks).

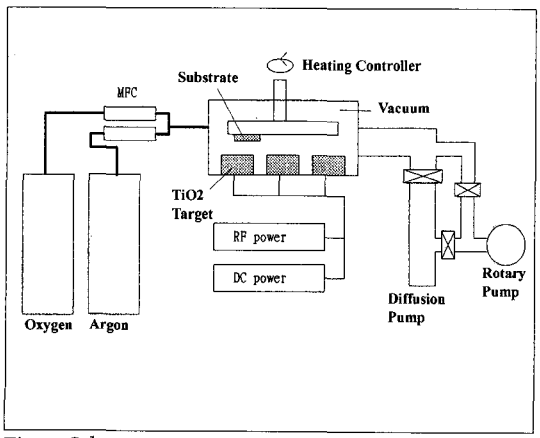

Fig. 1. Schematic diagram of RF magnetron sputtering system.

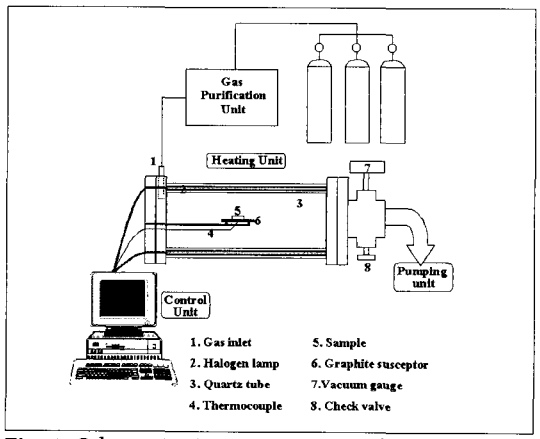

Fig. 2. Schematic diagram of rapid thermal annealing system.

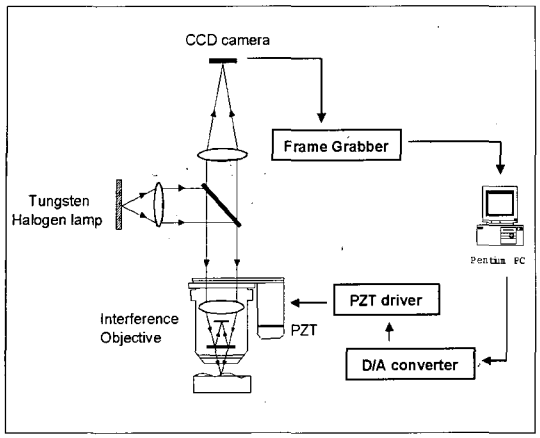

Fig. 3. Schematic diagram of optical interferometer.

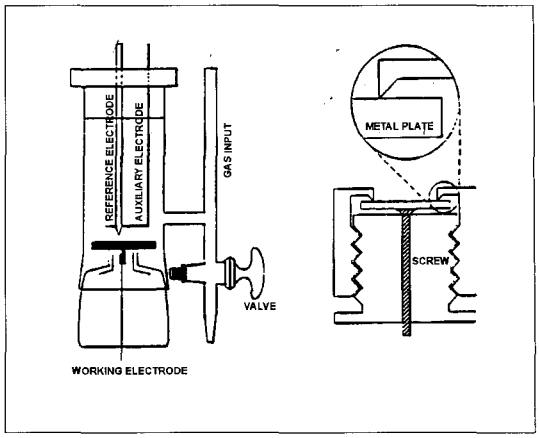

Fig. 4. Schematic diagram of potentiodynamic test.

2.1.3 XRD analysis

XRD analysis was performed to identify the surface composition and structure of the thermally treated samples. The instrument used was the Rotaflex RTP 300RE with a thin film attachment (Rigaku co. Japan), $2-\theta$ mode (2θ:10° ~70°) was used. The X-ray source was Cu-Kα, the tube voltage was 30 kV, the tube current was 20 mA and the scanning speed was 4° / min.

2.1.4 XPS analysis

Using the ESCALAB 220i spectrometer (VG Scientific Co.), each surface to be studied was irradiated with high-energy X-rays, creating an emission of the inner shell electrons of the atoms. All electrons whose binding energies were less than the energy of the exciting X-rays were ejected. The kinetic energy of these photoelectrons was measured with an electron energy analyzer. Because the energies of the excited electrons were very low, only those electrons originating in the few top monolayers could be detected, leading to a high surface sensitivity. The electrons originating far below the surface lost intensity because of the inelastic scattering effect, and remained in the background of the spectrum. To minimize further scattering, XPS analysis was performed (using the Al Kα X-ray) in an ultrahigh vacuum (10^{-8} torr).

2.1.5 Potentiodynamic curve

The flat cell (EG & E Co.) was used for potentiodynamic experiment (Fig. 4). The saturated calomel electrode (SCE) was used as the reference electrode, and platinum wire was used as counter electrode. The potential was scanned from 0.2 V below corrosion potential to 2 V, and the scan rate was 2 mV / sec.

2.2 Cell culture

For all experiments, cells were extracted from the femoral bone marrow of young adult rats, and were cultured on discs placed in 24 well plates (Nalge Nunc International). Controls consisted of cells cultured directly on the polystyrene surface of the 24 well plate. The cell were plated at 10,000 cells / discs in a α-minimal essential medium (α-MEM) containing 10% fetal bovine serum (FBS) and 1% antibiotic solution (diluted from a stock solution containing 5000 Uml^{-1} penicillin, and 5000 Uml^{-1} streptomycin: GIBCO. Grand Island, NY). The cultures were incubated at 37°C in an atmosphere of 100% humidity and 5% CO_2 (incubator from Forma. USA), and the media were changed every third day throughout the experiment.

2.3 Cell morphology

To determine whether cell morphology varied as

a function of the surface roughness and composition, the cultures were examined by scanning electron microscopy. The samples were harvested and the culture media were removed. The samples were then rinsed three times with Hank' s balanced salt solution (HBSS) and fixed with 1% OsO_4. After being fixed, the disks were rinsed with HBSS, sequentially incubated for 30-45 minutes each in 50, 75, 90 and 100 % ter-butyl alcohol, and vacuum dried. A thin layer of gold-palladium was sputter-coated onto the samples prior to examination in a JEOL JSM-840A cold field emission scanning microscope (JEOL Ltd. Akishima Tokyo, Japan).

2.4 Cell number

Upon harvesting, the cells were released from the culture surface by adding a mixture of 0.25% trypsin in Hank' s balanced salt solution (HBSS) and 1 mM ethylenediamine tetra-acetic acid (EDTA) for ten minutes at 37℃. The number of cells was determined with a Hemocytometer.

2.4.1 Cell attachment

The osteoblast-like cells were treated with a 0.05% Trypsin-0.02% EDTA solution and distributed, according to the number of 1×10^5 cell, to a 24 well plate with the Ti disc. During incubation the environment was maintained at 37℃, and 5% CO_2. The cell attachment level was counted with a hemocytometer after four hours, eight hours and 24 hours.

$$\% \text{ cell attachment} = \frac{\text{number of attached cell}}{\text{number of attached cell + number of unattached cell}}$$

2.4.2 Cell proliferation

The osteoblast-like cells were treated with a 0.05% Trypsin-0.02% EDTA solution and distributed, according to the number of 5×10^4 in 100 μl, to a 24 well plate with the Ti disc. After four hours in an incubator, the minimal essential medium (α- MEM) containing 10% fetal bovine serum and 1% antibiotics was supplemented. The cell proliferation level was counted with a hemocytometer after one day, three days and seven days.

2.5 Statistical Analysis

The microtopographical values of the optical interferometer were Ra, Rt and Rsk. Data were first analyzed by analysis of variance. When statistical differences were detected, the LSD (Least Significant Difference) was used, where $P < 0.05$ was considered significant. In the cell number test, each data point represented the mean of six individual cultures. Data were analyzed by ANOVA, LSD and, for non-parametric analysis, the Mann-Whitney test ($P < 0.05$).

RESULTS

3.1 Disc characteristics

- SEM of machined discs.

Typical machining grooves, as produced by the manufacturing instruments, were observed on the surface of the titanium discs (Fig. 5a).

- SEM of sandblasted discs.

The surface appeared glazed, and a very rough surface produced by the blasting procedure was observed. The surface was highly irregular, with many depressions and small indentations (Fig. 5b).

- SEM of thermal oxidation discs after TiO_2 sputter deposition.

In the 600℃ thermal oxidation group (Fig. 5c), the irregularities formed by the blasting procedure were masked by an oxide layer growth that looked like a lamella structure. In the 800℃ thermal oxidation group (Fig. 5d), continued oxide layer growth resulted in irregularities expecting mechanical strength. Looking at cross sections from each group, it was observed that the oxide layer was thicker in the 800℃ thermal oxidation group (Fig. 6).

Table I. Optical Interferometer Result

		Ra(㎛)	Rt(㎛)	Rsk
Machined	Mean	0.508[a]	5.897[a]	0.04[a]
	S.D.	0.102	0.695	0.197
Blasted	Mean	0.904[c]	15.218[b]	-0.0206[a]
	S.D.	0.060	2.459	0.277
S.600℃	Mean	0.869[c]	15.290[b]	0.389[b]
	S.D.	0.127	3.503	0.599
S.800℃	Mean	0.758[b]	15.387[b]	1.264[c]
	S.D.	0.112	3.116	0.908

a<b<c at P<0.05 (ANOVA and LSD test)

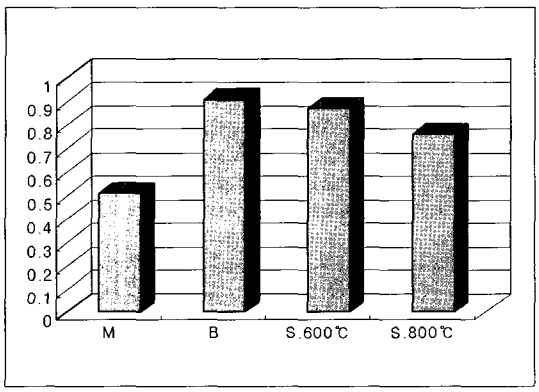

Fig. 7. The effect of surface treatment on surface roughness(Ra, ㎛).

3.1.1 Surface roughness

Table I and Fig. 7-8 show the results of the optical interferometer analyses.

1. The lowest surface roughness was observed in the machined group (Ra value=0.508㎛) and the highest was in the blasting group (Ra value=0.904 ㎛). The thermal oxidation procedure reduced surface roughness (ANOVA, LSD P<0.05).
2. There was no significant difference in the Ra values of the blasting group and 600℃ thermal oxidation group. The Ra value of the 800℃ thermal oxidation group was significantly lower than that of the blasting group (ANOVA, LSD P<0.05).
3. The Rt values of the blasting and thermal oxidation groups were significantly higher than that of machined group (ANOVA, LSD P<0.05).
4. The Rsk value of the 800℃ thermal oxidation group was unique, showing a much higher positive shift.

3.1.2 XRD

In the machined and blasting groups, the X-ray diffraction spectroscopy expressed only a Ti peak. Since the titanium surface in air conditions has a naturally-formed very thin oxide layer about 5 nm thick, which is not detected by XRD, there was no TiO_2 peak in the XRD pattern (Fig. 9). After TiO_2 sputter deposition and thermal oxidation, the TiO_2 layer thickness and crystallinity increased (Fig. 10).

In the XRD pattern, the overall TiO_2 peak was higher in the 800℃ thermal oxidation group than in the 600℃ thermal oxidation group. Looking at the TiO_2 crystallinity, increased rutile form was outstanding in the 800℃ thermal oxidation group. The anatase form increased slightly due to TiO_2 sputter deposition and thermal oxidation.

3.1.3 XPS

Fig. 11 shows the XPS pattern of the 800℃ thermal oxidation group. All of the surface Ti was bound with oxygen, and there was no contamination attrib-

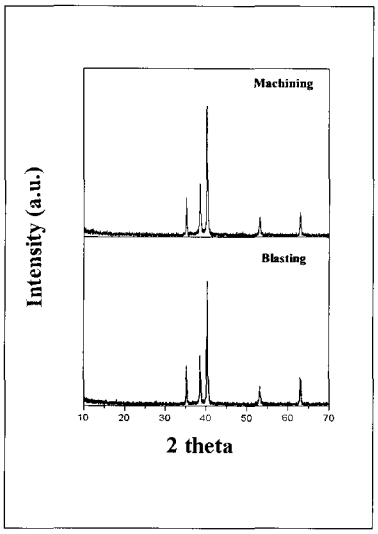

Fig. 9. XRD pattern of mach-ined, blasted group.

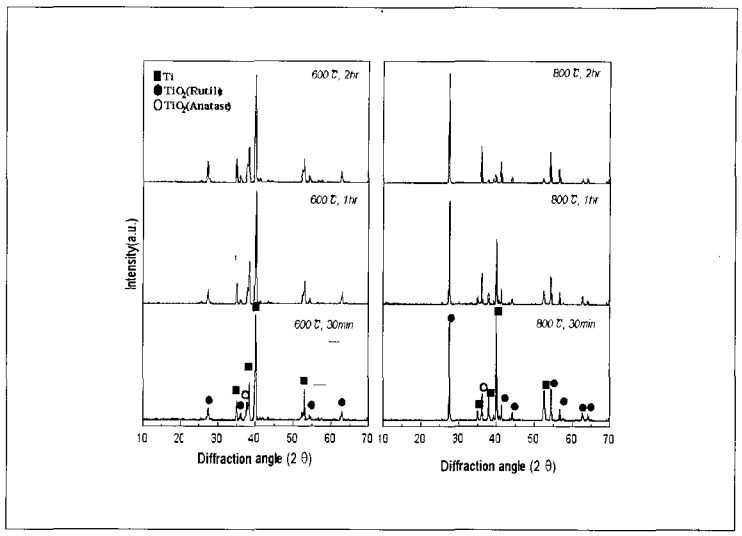

Fig. 10. XRD pattern of TiO_2 sputtering and thermal oxidation.

Table II. Percent cell attachment level (%±S.D.)

	4hr	8hr	24hr
Machined	$17.6^{a}\pm8.7$	$41.3^{a}\pm7.9$	$67.6^{b}\pm9.6$
Blasted	$36.5^{b}\pm5.6$	$49.4^{a}\pm15.0$	$50.6^{a}\pm9.4$
S.600℃	$70.8^{c}\pm9.2$	$74.5^{b}\pm10.3$	$64.7^{b}\pm16.9$
S.800℃	$38.5^{b}\pm19.2$	$49.3^{a}\pm14.2$	$51.5^{a}\pm12.2$

n=6. a<b<c at p=0.05(ANOVA, LSD and Mann-whitney)

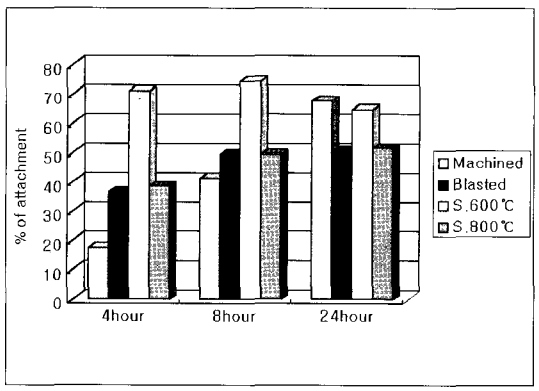

Fig. 14. Percent of cell attachment level.

uted to the fact that the thermal oxidation was carried out in a pure oxygen environment. The XPS analysis revealed that the oxygen binding state of titanium was TiO_2 or TiO. The TiO may be generated from the destruction of Ti-O binding in the TiO_2 layer by an argon beam sputter during the procedure. This means that the biocompatibility of the TiO_2 layer can be acquired through thermal oxidation in a pure oxygen environment.

3.1.4 Potentiodynamic polarization curves

Fig. 12 shows the polarization curve of the TiO_2/Ti samples in 0.15 M NaCl solution. In the graph of non-treated Ti, the current density was nearly constant in some potential range (-0.2V~1.5V), which is characteristic of the so-called valve-metal behavior of titanium. The current density was about 1×10^{-5} A/cm^2, and is significantly lower value in metals. In blasted sample, an increased potential resulted in pitting, and the pitting current increased to 10^{-3}A/cm^2. TiO_2 sputtering with the thermal oxidation samples showed better corrosion resisting properties. Pitting currents of the groups that underwent sputtering and heat treatments at 600℃ and 800℃ were 10^{-4}A/cm^2 and 10^{-5}A/cm^2, respectively, which means that the

Table III. Cell proliferation ($\times 10^4$mean±S.D.)

	1day	3day	7day
Machined	0.87±0.41	6.57±1.80	12.63±3.06
Blasted	2.00±0.42	7.03±1.19	14.17±3.52
S.600℃	1.83±0.57	7.10±1.85	11.80±3.00
S.800℃	1.67±0.43	4.07±1.16	11.47±3.14

*=singnificant difference at $p<0.05$(ANOVA and LSD)

sample treated at 800℃ has better anti-corrosion properties than the sample treated at 600℃.

3.2 Cell morphology

The appearance of the cells varied with surface roughness and chemical composition of the discs. The cells that grew on the machined surface were along the groove as a monolayer. The cells had an elongated dendritic appearance, where the extensions connected with others. In the cultures on the blasting and oxidation surfaces, the cells grew in multiple layers in a cuboidal shape with a long dendritic appearance (Fig. 13).

3.3 Cell number

3.3.1 Cell attachment

At the four-hour and eight-hour marks, the percent attachment level of the 600℃ thermal oxidation group was higher than that of the others ($P<0.05$). After 24 hours, there was no significant difference between the attachment levels of the groups. It is interesting to note that there was a consistently similar pattern between the blasting group and the 800℃ thermal oxidation group (Table Ⅱ, Fig. 14).

3.3.2 Cell proliferation

Taking measurements on days one, three and seven, the cell proliferation pattern was observed to be quite similar among all the groups ($P<0.05$)(Table Ⅲ, Fig. 15).

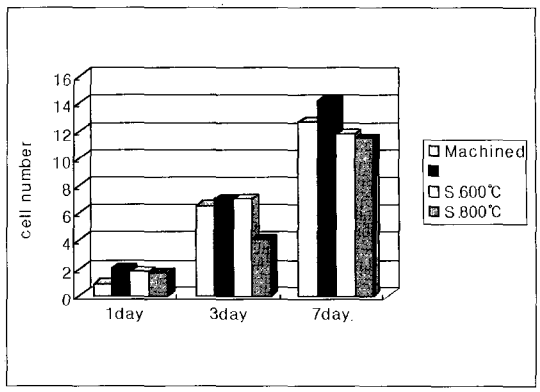

Fig. 15. Cell proliferation ($\times 10^4$).

DISCUSSION

This study was performed to evaluate the previous observations that osteoblast-like cells respond in a differential manner to both surface roughness[14,15] and material composition.[16] Cell culture may be used to investigate the surface-dependent responses of bone-forming cells.[17] The surface topographic features of commercially pure titanium substrates can alter the extracellular matrix formation and mineralization of cultured osteoblasts. Similar molecular and cellular assessments of in vivo responses to implant surface topography may contribute to improved engineering of endosseous implants. Understanding the relationships between material surface properties, adsorbed proteins, and cellular responses is essential to designing optimal material surfaces for implantation and tissue engineering.[18]

In the cell proliferation experiment, there was no difference among the groups throughout. This result supports the notion that roughness may play a more important role in determining cell response than the type of topography, as long as the Ra values can be sensed by the cells. Kieswetter,[19] Lyndon[20] and Martin[21] reported that there was an inverse relationship between cell number and the Ti surface roughness. Stanford mentioned that, on a per-cell ba-

sis, the levels of the bone-specific protein, osteocalcin, and the enzymatic activity of alkaline phosphatase were highest on the smooth 1-micron polished surface, and were lowest on the roughest surfaces for the plasma-cleaned cpTi. Lincks[22] stated that the optimal surface appeared to be one with an Ra value of around 4μm, such that the cell proliferation was reduced but not blocked and the phenotypic differentiation was enhanced, and that this roughness can be gained by blasting.

Adriano,[23] Degasne,[24] Bowers[25] and Ong[26] said that significantly higher levels of cellular attachment were found using rough, sandblasted surfaces with irregular morphology. Qu[27] stated that a grooved surface permitted the attachment of more cells than a smooth one. Cell shape and cytoskeleton were strikingly influenced as early as 20 minutes after cell attachment, when the cytoskeleton begins to align with the topography.

The morphology of the cells on the oxidized surface demonstrates that they have assumed a more cuboidal shape with dendritic extensions, typical of a more differentiated osteoblast. In contrast, cells on the smoother surfaces appeared more flattened and fibroblastic. Scanning electron microscopy examination revealed that the osteoblasts cultured on implant metals synthesized and deposited an extracellular matrix containing collagenous and noncollagenous components, as well as mineral nodules of various morphologies. The bulk of the osteoblast mineral deposits was amorphous hydroxyapatite. In addition, electron diffraction analysis revealed small regions of crystalline hydroxyapatite.[28]

Though a titanium oxide layer formed on each disc surface, it is unlikely that the oxides were identical. The TiO_2 sputter deposition and O_2 annealing procedures by thermal oxidation in various manner will differentiate the oxide thickness and crystallinity. This would have a direct effect on the nature of the conditioning film that forms as the material surface interacts with the culture medium.[29] In addition, ions released from the titanium surface could also modulate the cellular response. The protein adsorption events are necessary to control the attachment and subsequent spatial distribution of the bone-derived cells exposed to the chemically modified surfaces.[30] In our experiment, the surface of the 600℃ thermal oxidation group may have a microtopography that easily bound protein substrates in the culture media because of a high level of initial cell attachment.

The composite effects of surface energy, composition, roughness and topography plays a major role during the initial phases of the biological response to the implant, such as protein adsorption and cellular adherence, as well as during the later and more chronic phases of the response. For bone, the successful incorporation (and hence the rigid fixation) of an alloplastic material within the surrounding bony bed is called osteointegration. The exact surface characteristics necessary for optimal osteointegration, however, remain to be elucidated

In the case of osteointegration, if the implant surface is inappropriate or less than optimal, cells will be unable to produce the appropriate complement of autocrine and paracrine factors required for the adequate stimulation of osteogenesis at the implant site. In contrast, if the surface is appropriate, the cells at the implant surface will stimulate interactions between the cells at the surface and those in the distal tissues. This, in turn, will initiate a timely sequence of events which include cell proliferation, differentiation, matrix synthesis, and local factor production, thereby resulting in the successful incorporation of the implant into the surrounding bony tissue.[31]

CONCLUSIONS

1. Surface roughness values were, from the lowest to the highest, machined group, 800℃ thermal oxidation group, 600℃ thermal oxidation group and blasting group. The Ra value of blasting group was significantly higher than that of 800℃ thermal oxidation group (P=0.003), which was not different

from that of 600℃ thermal oxidation group (P=0.345).

2. The microtopographic profile of the 800℃ thermal oxidation group showed a positive shift of Rsk, which was significantly different from other groups (P=0.000).
3. The thickness and crystallinity of the TiO_2 layer were higher in the 800℃ thermal oxidation group than in the 600℃ thermal oxidation group.
4. The degree of cell attachment was highest in the 600℃ thermal oxidation group after four and eight hours (P<0.05), but after 24 hours, there was no difference among the groups .
5. The level of cell proliferation showed no difference among the groups after one day, three days and seven days.

REFERENCES

1. Rich A, Harris AK. Anomalous preferences of cultures macrophages for hydrophobic and roughened substrata. J Cell Sci 1981;50:1-7.
2. Thomas K, Cook SD. An evaluation of variables influencing implant fixation and direct bone apposition. J Biomed Mater Res 1985;19:875-901.
3. Schroeder A, Van der Zypen E, Stich H, Sutter F. The reactions of bone, connective and epithelium to endosteal implants with titanium sprayed surfaces. J Maxillofac Surg 1981;9:15-25.
4. Buser D, Schenk R, Steinemann S, Riorellini J, Fox C, Stich H. Influence of surface characteristics on bone integration of titanium implants. A histomorphometric study in miniature pigs. J Biomed Mater Res 1991;25:889-902.
5. Cochran DL, Simpson J, Weber H, Buser D. Attachment and growth of periodontal cells on smooth and rough titanium. Int J Oral Maxillofac Implants 1994;9:289-976.
6. Michaels CM, Keller JC, Stanford CM, Solursh M. In vitro cell attachment of osteoblast-like cells to titanium. J Dent Res 1989;68:276.
7. Bowers KT, Keller JC, Randolph BA, Wick DG, Michaels CM. Optimization of surface micromorphology for enhanced osteoblast responses in vitro. Int J Oral Maxillofac Implants 1992 Fall;7(3):302-10.
8. Martin JY, Schwartz Z. Effect of titanium surface roughness on proliferation, differentiation, and protein synthesis of human osteoblast-like cells (MG63). J Biomed Mater Res 1995 Mar;29(3):389-401.
9. Boyan BD, Batzer R, Kieswetter K, Liu Y, Cochran DL, Szmuckler-Moncler S, Dean DD, Schwartz Z. Titanium surface roughness alters responsiveness of MG63 osteoblast-like cells to 1α, 25-(OH)2D3. J Biomed Mat Res 1998;39:77-85.
10. Cheroudi B, Gould TRL, Brunette DM. Titanium-coated micro-machined grooves of different dimensions affect epithelial and connective tissue cells differently in vivo. J Biomed Mater Res 1990;24:1203-19.
11. Brunette DM. The effects of implant surface topography on the behavior of cells. Int J Oral Maxillofac Implants 1988;3:231-46.
12. Golijanin L, Bernard G. Biocompatibility of implant metals in bone tissue culture. J Dent Res 1988;67:367.
13. Nowlin P, Carnes D, Windeler A. Biocompatibility of dental implant materials sputtered onto cell culture dishes. J Dent Res 1989;68:275.
14. Groessner-Schreiber b, Tuan RS. Enhanced extracellular matrix production and mineralization by osteoblasts cultured on titanium surfaces in vitro. J Cell Sci 1992;101:209-17.
15. Ong JL, Prince CW, Raikar GN, Lucas LC. Effect of surface topography of titanium on surface chemistry and cellular response. Implant Dent 1996 Summer;5(2):83-8.
16. Braun G, Kohavi D, Amir D, Luna MH, Caloss R, Sela J, Dean DD, Boyan BD, Schwartx X. Markers of primary mineralization are correlated with bone-bonding ability of titanium or stainless steel in vivo. Clin Oral Implants Res 1995;6:1-13.
17. Cooper LF, Masuda T, Whitson SW, Yliheikkila P, Felton DA. Formation of mineralizing osteoblast cultures on machined, titanium oxide grit-blasted, and plasma-sprayed titanium surfaces. Int J Oral Maxillofac Implants 1999 Jan-Feb;14(1):37-47.
18. Webb K, Hlady V, Tresco PA. Relative importance of surface wettability and charged functional groups on NIH 3T3 fibroblast attachment, spreading, and cytoskeletal organization. J Biomed Mater Res 1998 Sep 5;41(3):422-30.
19. Kieswetter K, Schwartz Z. Surface roughness modulates the local production of growth factors and cytokines by osteoblast-like MG-63 cells. J Biomed Mater Res 1996 Sep;32(1):55-63.
20. Lyndon f. Cooper, Takayufi Masuda. Formation of Mineralizing osteoblast cultures on machined, Titanium oxide Grit- Blasted, and plasma-sprayed titanium surfaces. Int J Oral Maxillofac Implants 1999;14:37-47.
21. Martin JY, Schwartz Z. Effect of titanium surface roughness on proliferation, differentiation, and protein synthesis of human osteoblast-like cells (MG63). J Biomed Mater Res 1995 Mar;29(3):389-401.
22. J.Lincks. Response of MG63 osteoblast-like cells to titanium and titanium alloy is dependent on surface roughness and composition. Biomaterials 1998;19:2219-2232.
23. Adriano Piattelli. Histologic and Histom-orphometric Analysis of the Bone response to machined

and sandblasted titanium implants: An experimental study in rabbits. Int J Oral Maxillofac Implants 1998;13:805-810.
24. Degasne I, Basle MF. Effects of roughness, fibronectin and vitronectin on attachment, spreading, and proliferation of human osteoblast-like cells (Saos-2) on titanium surfaces. Calcif Tissue Int 1999 Jun;64(6): 499-507.
25. Bowers KT, Keller JC, Randolph BA, Wick DG, Michaels CM. Optimization of surface micromorphology for enhanced osteoblast responses in vitro. Int J Oral Maxillofac Implants 1992 Fall;7(3):302-10.
26. J.L.Ong. Surface roughness of titanium on bone morphogenetic protein-2 treated osteoblast cells in vitro. Implant Dent 1997;6:19-24.
27. Qu J, Chehroudi B, Brunette DM. The use of micromachined surfaces to investigate the cell behavioral factors essential to osseointegration. Oral Dis 1996 Mar;2(1):102-15.
28. Squire MW, Ricci JL, Bizios R. Analysis of osteoblast mineral deposits on orthopaedic/ dental implant metals. Biomaterials 1996 Apr;17(7):725-33.
29. Norde W. Behavior of proteins at the interfaces, with special attention to the role of the structure stability of the protein molecule. Clin Mater 1998;11:85-91.
30. Thomas CH, McFarland CD. The role of vitronectin in the attachment and spatial distribution of bone-derived cells on materials with patterned surface chemistry. J Biomed Mater Res 1997 Oct;37(1):81-93.
31. Kieswetter K, Schwartz Z, Dean DD, Boyan BD. The role of implant surface characteristics in the healing of bone. Crit Rev Oral Biol Med 1996;7(4):329-45.

Reprint request to:
Dr. Seong-Joo Heo
Dept. of Prosthodontics, College of Dentisity,
Seoul National Univ.
28-1 Yeongun-Dong, Chongno-Gu, 110-749, Seoul Korea
heosj@plaza.snu.ac.kr

EXPLANATION OF PHOTOGRAPHY

Fig. 5a. SEM of machined surface (×700, 3500).
Fig. 5b. SEM of blasted surface (×700, 3500).
Fig. 5c. SEM of 600℃ thermal oxidation surface with TiO_2 sputtering (×700, 3500).
Fig. 5d. SEM of 800℃ thermal oxidation surface with TiO_2 sputtering (×700, 3500).
Fig. 6a. SEM of sectioning surface : 600℃ thermal oxidation surface with TiO_2 sputtering (×6000)
Fig. 6b. SEM of sectioning surface : 800℃ thermal oxidation surface with TiO_2 sputtering (×3000)
Fig. 8a. Microtopography of machined surface.
Fig. 8b. Microtopography of blasted surface.
Fig. 8c. Microtopography of 600℃ thermal oxidation surface with TiO_2 sputtering.
Fig. 8d. Microtopography of 800℃ thermal oxidation surface with TiO_2 sputtering.
Fig. 11. XPS pattern of 800℃ thermal oxidation group.
Fig. 12. Potentiodynamic curve of machined, blasted, S.600℃ and S.800℃ Ti disc.
Fig. 13a. SEM of cell morphology : machined surface at 1 day (×700).
Fig. 13b. SEM of cell morphology : blasted surface at 1 day (×700).
Fig. 13c. SEM of cell morphology : S.600℃ at 1 day (×700).
Fig. 13d SEM of cell morphology : S.800℃ at 1 day (×700).

FIGURES ①

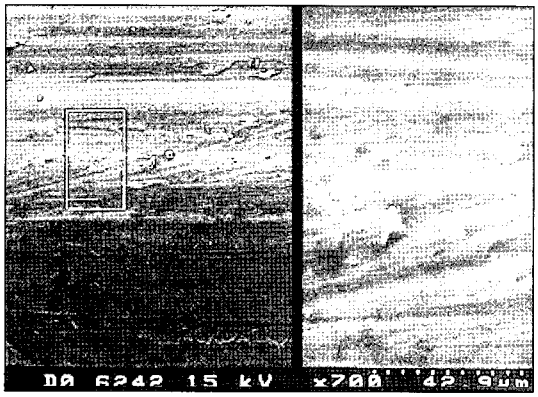

Fig. 5a

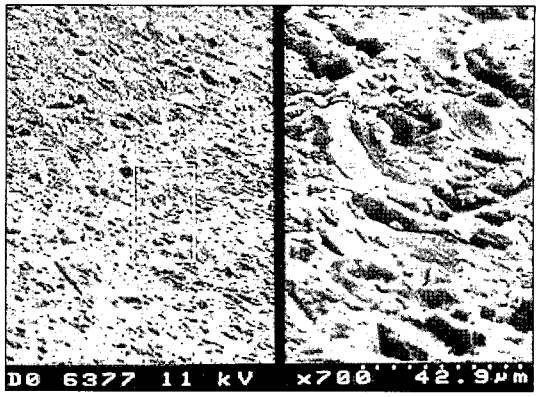

Fig. 5b

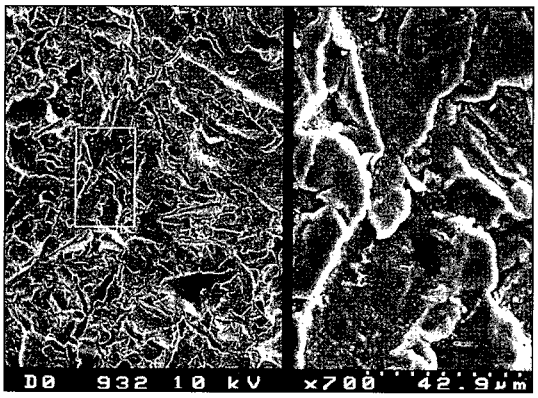

Fig. 5c

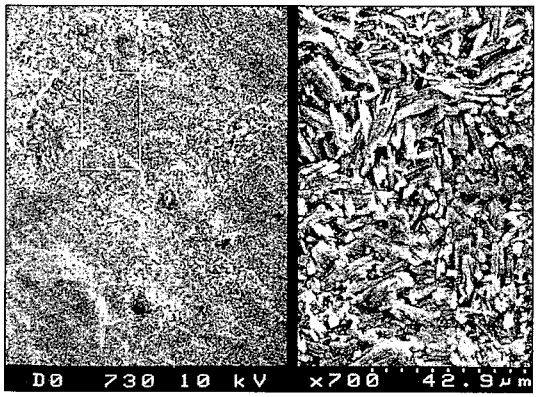

Fig. 5d

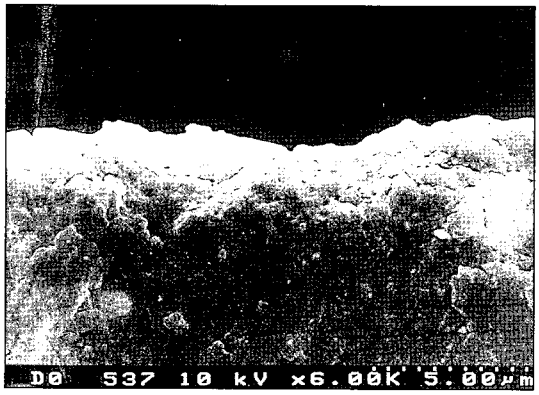

Fig. 6a

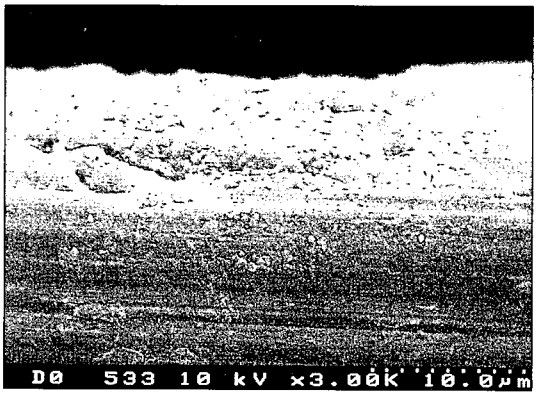

Fig. 6b

FIGURES ②

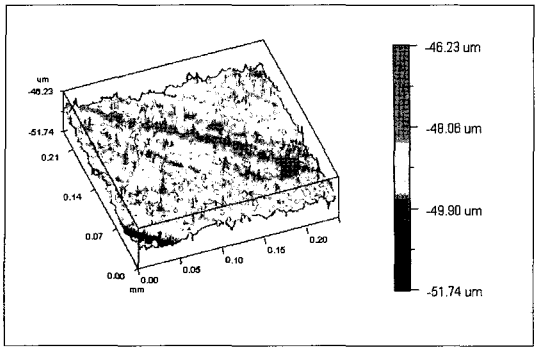

Fig. 8a

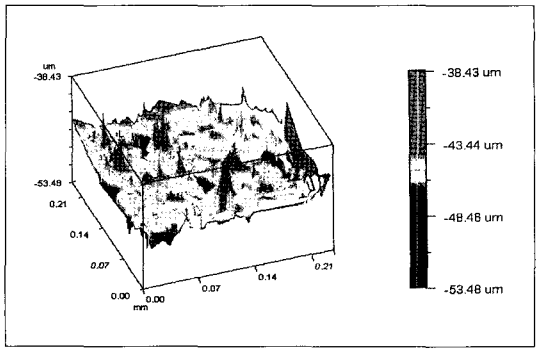

Fig. 8b

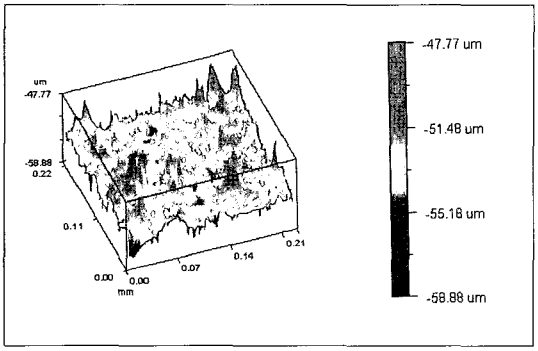

Fig. 8c

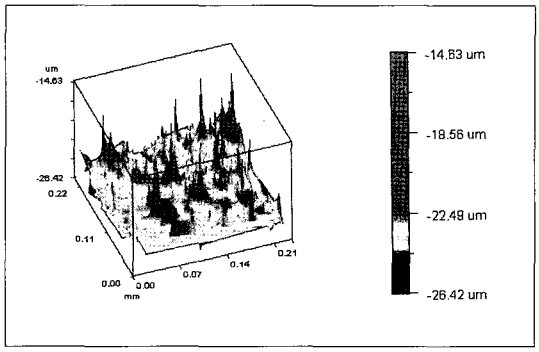

Fig. 8d

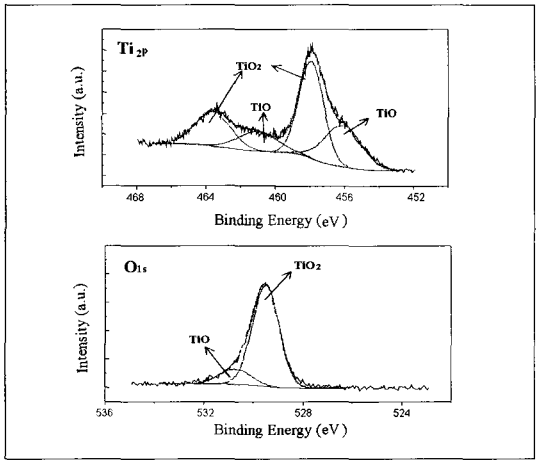

Fig. 11

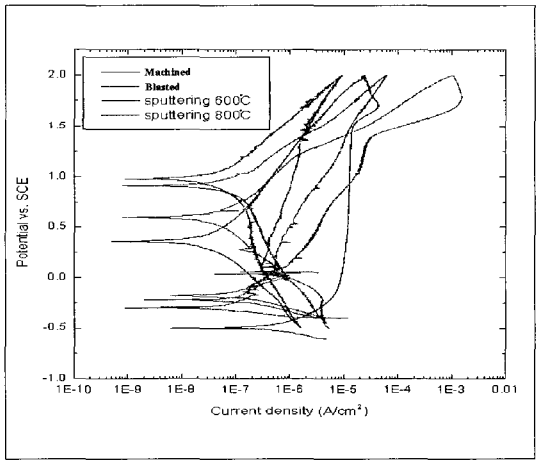

Fig. 12

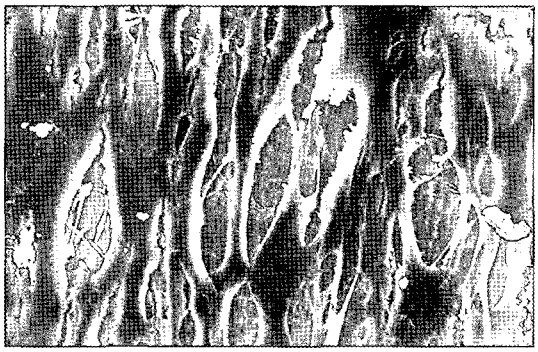

Fig. 13a

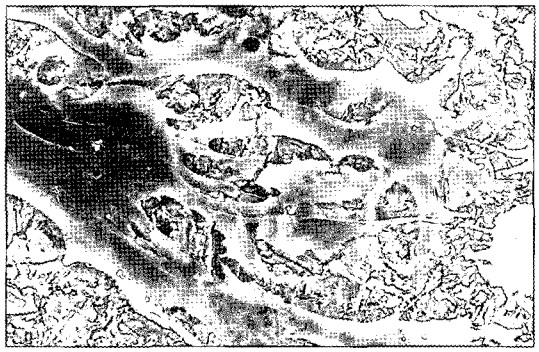

Fig. 13b

Fig. 13c

Fig. 13d